A Cardiovascular Model for the Analysis of Pacing Configurations in Cardiac Resynchronization Therapy

K Tse Ve Koon[1,2], V Le Rolle[1,2] , G Carrault[1,2] , A I Hernández[1,2]

[1]Université de Rennes 1, LTSI, Rennes, F-35000, France
[2]INSERM, U642, Rennes, F-35000, France

Abstract

A lumped-parameter model of the cardiovascular system, made of 3 interacting modules (an electrical heart model, an elastance-based mechanical heart model and a circulatory system) is proposed in this paper. This model is able to reproduce the clinically observed quasi-parabolic nature of the dependence of systolic blood pressure (SBP) on atrioventricular (AVD) and interventricular (VVD) delays and the increased SBP on AVD dependance at high heart rates. A sensitivity analysis has been performed on the main variables of this model, as well as parameter identification on interpolated clinical data. Results from these analyses show the importance of integrating the circulatory and regulatory systems for the reproduction of appropriate physiological responses to CRT.

1. Introduction

Cardiac resynchronization therapy (CRT) is widely applied to patients suffering from chronic heart failure, meeting specific criteria [1]. However, among patients selected for CRT, around 30% are non-respondents. A possible reason for this is that the atrioventricular (AVD) and interventricular (VVD) pacing delays are not correctly optimized. One of the possible non-invasive optimization targets, systolic blood pressure (SBP), has been shown to exhibit an optimal AVD and VVD configuration with a pseudo-parabolic variation for both; the curvature for the former being more pronounced [2, 3]. In addition, higher heart rates induce increased SBP(AVD) dependance. The aim of this work is to propose a mathematical model of the cardiovascular system reproducing these main hemodynamic effects resulting from changes in AVD and VVD during CRT. In the first part of this paper, we describe the model used, before investigating possible causes for the increased SBP(AVD) dependance at higher heart rates. Finally, parameter identification is carried out by minimizing a cost function defined between the model output and a set of interpolated clinical data.

2. Model description

The system model used in this paper is composed of a pacemaker, an electrical heart, a mechanical heart and a circulatory system as schematically described in fig. 1.

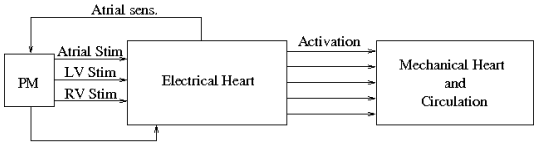

Figure 1. System model.

2.1. Electrical heart model

The electrical heart model is based on a previous work proposed in our laboratory [4]. It is made of two types of adaptive automata representing different cardiac structures. The seven nodal automata represent the sinoatrial node atrioventricular node, upper and lower bundle of His, left and right bundle branches and left and right septal bundle branches, while the five myocardial automata represent the left and right atria, left and right ventricles and the interventricular septum. The model has four inputs; the heart rate (HR) which is fed directly to the sinoatrial node and three stimulation inputs coming from the pacemaker ($Stim.A$, $Stim.RV$ and $Stim.LV$) simulating the three pacing leads used in CRT. The model then sends five activation signals which are fed to the mechanical heart model; a sixth output representing the atrial sensing is also sent to the pacemaker model.

2.2. Circulatory and mechanical models

The mechanical heart model is embedded into the circulatory model, as shown in fig. 2. The mechanical heart model is composed of four chambers, representing atria and ventricles, and one artificial volume, associated with the interventricular septum, as proposed by [5,6]. The right ventricle and left atrium are connected via the pulmonary circulation while blood flows from the left ventricle to the

right atrium through the systemic circulation. For both of these circulations, lumped-parameter models have been chosen. Resistances (R) simulate pressure gradients due to resistances encountered by blood passing through the different sections. Inductors (L) describe inertial effects due to changes in the velocity of blood flow and finally, capacitors (C) are included since blood can be stored in the different vessels. Parameter values for these elements are given in fig.2. Four diodes have been included to represent the aortic, tricuspid, pulmonary and mitral valves. These diodes have been assigned a resistance of 0.01 in forward bias and $100\ mmHg.s/ml$ in reverse bias.

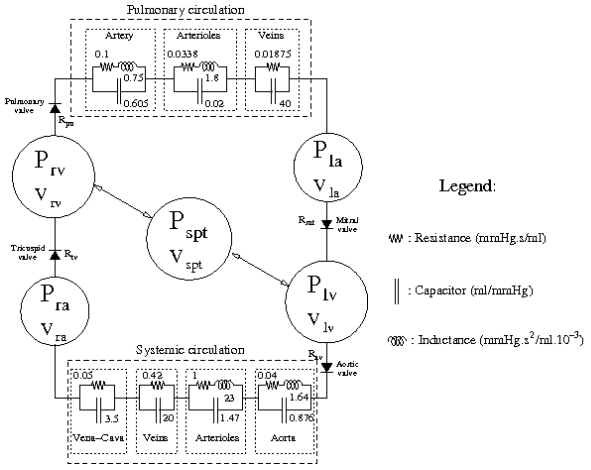

Figure 2. Circulatory and mechanical heart model.

2.3. Atrial and ventricular activities

The dynamics of atria and ventricles are described by elastic chambers. One cycle of the atrial elastance is given by:

$$E_a(t) = E_{a,max}\left[e_a(t) + \frac{E_{a,min}}{E_{a,max}}\right], \qquad (1)$$

$e(t)$ being the driver function. In the present paper, a gaussian function was chosen [7]:

$$e_a(t) = exp\left[-B_a.\left(\frac{HR}{80}\right)^2.\left(t - C_a\left(\frac{80}{HR}\right)\right)^2\right], \quad (2)$$

B_a and C_a are parameters equal to $180\ s^{-2}$ and $0.2\ s$ respectively. These values are chosen for a reference heart rate (HR) of 80 beats per minute (bpm).

As for the ventricles, one can identify two main characteristics in their PV cycles, namely the end systolic pressure-volume relationship (ESPVR) and the end diastolic pressure-volume relationship (EDPVR), which define, respectively, the upper and lower bounds of the loops. These two relationships can be written as follows [8]:

$$P_{es} = E_{es}\left(V - V_0\right), \qquad (3)$$

$$P_{ed} = P_0\left(e^{\lambda(V-V_0)} - 1\right). \qquad (4)$$

Eq. (3) describes the linear relationship between end systolic pressure (P_{es}), volume (V), volume at zero pressure (V_0) and elastance (E_{es}), while eq. (4) defines the non-linear relationship between end diastolic pressure (P_{ed}) and volume (V); P_0, λ and V_0 being the related parameters. The pressure of anyone ventricle can finally be written in terms of equations (3) and (4) and its driver function ($e_v(t)$):

$$P_v(V,t) = e_v(t)P_{es} + (1 - e_v(t))P_{ed}. \qquad (5)$$

The driver function for the ventricles are similar to the one used for the atria, except for parameters B_v and C_v which are different reflecting longer ventricular contractions (with respect to atrial contractions). Throughout this paper, we have set B_v and C_v equal to $112\ s^{-2}$ and $0.26\ s$ respectively.

2.4. Interventricular coupling

The two ventricles are made to interact through the interventricular septum. Following Smith's model [5, 6] the left and right ventricular free wall volumes read:

$$V_{lvf} = V_{lv} - V_{spt}, \qquad (6)$$

$$V_{rvf} = V_{rv} + V_{spt}, \qquad (7)$$

where V_{spt} represents the modification on both V_{lvf} and V_{rvf} due to septal dynamics. Pressures for the ventricles and septum are in the same form as eq.(5):

$$\begin{aligned} P_{lvf} &= e_{lvf}(t)P_{es,lvf} + (1 - e_{lvf}(t))P_{ed,lvf} \\ P_{rvf} &= e_{rvf}(t)P_{es,rvf} + (1 - e_{rvf}(t))P_{ed,rvf} \\ P_{spt} &= e_{spt}(t)P_{es,spt} + (1 - e_{spt}(t))P_{ed,spt} \end{aligned}$$

and are interelated as follows:

$$P_{spt} = P_{lvf} - P_{rvf}. \qquad (8)$$

The complete model has been developed using *Simulink*^{TM} and the next sections discuss results obtained from this model.

3. Simulation results

Fig. 3 shows an example of simulated pressures and left ventricular volume obtained from our model. The signals correspond to a stationnary state reached by the model after an initial transient regime. To obtain a complete AVD/VVD scanning, for each pacing configuration, the

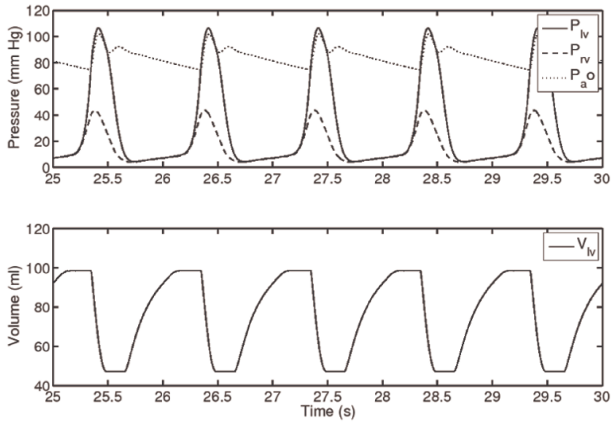

Figure 3. Simulated pressures and volume obtained from our model at 60 bpm.

model is run for 30 s and values for pressures are recorded during the last 6 s, where a stationnary state is reached. Fig. 4 shows the simulated steady-state values of SBP_{rel}, obtained from the model at 60 bpm, by scanning $AVDs$ and $VVDs$ (range $[40, 200]$ and $[-40, 40]$ respectively). Here, SBP_{rel} represents a relative SBP value with respect to a reference configuration ($AVD = 120\ ms$ and $VVD = 0\ ms$), as done by Whinnett et al. [2, 3]. As can be seen the SBP_{rel} curve exhibits an optimal AVD and VVD point. In this model, the value of the former depends mainly on the synchronization between atrial and ventricular contraction (preload condition) as seen during echocardiography [9] while the latter depends mainly on the Upstroke Activation Period (UAP) values for ventricles and septum. These values correspond to the delay between electrical and mechanical activations. In order to reproduce the modifications of SBP_{rel} observed for higher heart rates (typically 110 bpm), we have considered four different physiological changes to our model which are heart rate dependent:

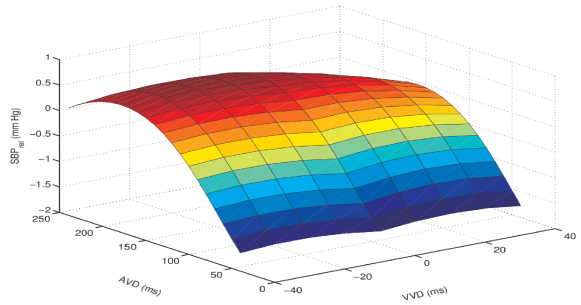

Figure 4. AVD and VVD scanning performed at 60 bpm.

1. Increase in contractility for the left and right ventricles and the septum (done by increasing E_{es} values).
2. Pulmonary vasodilation, resulting in decreased resistance values for the pulmonary artery and arterioles.
3. Systemic vasodilation, leading to decreased resistance values in the systemic arterioles.
4. Venous regulation, which induces reduced capacitance values for the pulmonary and systemic veins.

To evaluate the consequences of these changes on the dependence of SBP_{rel} on AVD at higher HR, we have carried out a sensitivity analysis, by associating a gain term with each one of these effects. Results of this analysis are displayed in fig. 5. The amplitude of variation of SBP_{rel} with respect to AVD variations ($[40, 200]\ ms$) at 110 bpm is plotted vs different gain values. As can be seen, venous regulation is the leading effect explaining the clinically observed trend, the other three induce changes opposite to what is required. While integrating these changes in the model, we carried out further simulations at higher HR (110 bpm) so as to plot the SBP_{rel} variations with AVD and VVD. At such HR [3], the variation of SBP_{rel} with AVD is more pronounced than at lower HR and there is a shortening of the optimal AVD pacing configuration, which is consistent with clinical observations [3].

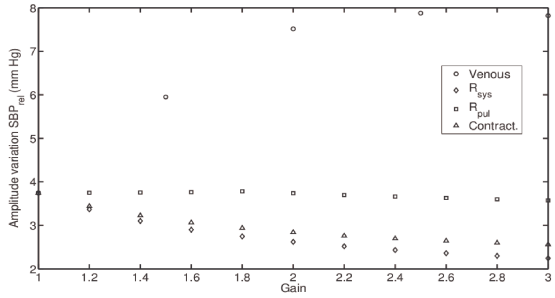

Figure 5. Variation of SBP_{rel} with AVD at 110 bpm with increasing gain values for four different effects.

4. Parameter identification

It is now necessary to confront our model to clinical data. Unfortunately, such data is unavailable and we have instead used results published by Whinnett et al [2]. The latter reported that among their cohort, variations of SBP_{rel} with AVD and VVD fitted closely to a parabola with the former being significantly more curved; average quadratic coefficients -1194 and $-670\ mmHgs^{-2}$ respectively. To simulate these observations, three optimal AVD/VVD configurations have been tested; $100/0, 110/-10$ and $90/20$; and for each of them, the two central lines of the bell-shaped curves have been interpolated i.e. $SBP_{rel}(AVD)(AVD \in$ [40:10:200] ms and $VVD = 0\ ms$) and $SBP_{rel}(VVD)(VVD \in$ [-40:10:40] ms and $AVD = 120\ ms$). An evolutionnary algoritm [10] is then applied with the error function defined as the relative mean squared error (rMSE) between the model output and the interpolated clinical data. The parameters concerned by this procedure are:

- for the atrial elastance :$E_{a,max}$, $E_{a,min}$, and C_a
- three elastance parameters for the ventricles and septum: E_{es}, P_0 and λ (different for each chamber)
- gain values for contractility (different for each chamber), venous regulation, systemic and pulmonary resistance.
- UAP values for ventricles and septum.

The procedure yields the set of parameters minimizing the rMSEs which read 0.111, 0.096 and 0.114 for the above-mentionned optimal configurations. In fig. 6(a) we compare, for the first configuration, the interpolated and simulated data while figure 6(b) shows the corresponding complete AVD/VVD scanning results.

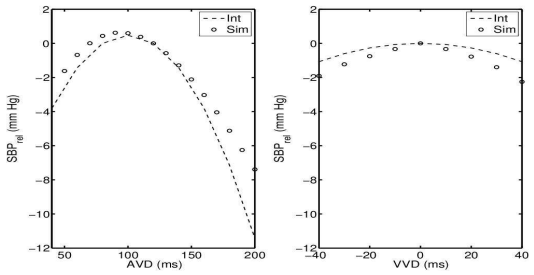

(a)

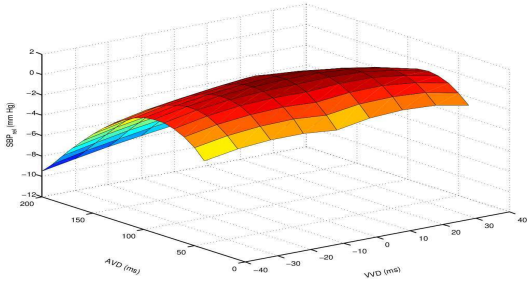

(b)

Figure 6. (a) Comparison between interpolated clinical data (dash) and simulation results (circles) for $SBP_{rel}(AVD)$ at $VVD = 0\ ms$ (left) and $SBP_{rel}(VVD)$ at $AVD = 120\ ms$ (right) for an optimal configuration of $AVD = 100\ ms$ and $VVD = 0\ ms$ and (b) AVD/VVD scanning results of the simulations.

5. Conclusion

We have proposed a lumped-parameter model of the cardiovascular system, capable of generating a quasi-parabolic dependence of SBP_{rel} with respect to the AVD and VVD pacing parameters. Although appropriate clinical datasets are still required to complete the validation of the model, obtained results are encouraging and show the importance of taking into account the interactions between electrical, mechanical and hemodynamic phenomena, in order to analyze the consequences of different pacing parameters on CRT. The inclusion of a regulatory system reveals to be fundamental for studying CRT response to varying HRs and, although a model of short-term autonomic regulation has not being integrated yet in this model, the obtained results will certainly serve in this sense. In its current state, the model can be employed in developing and testing CRT pacing parameters optimization algorithms, functioning in a continuous fashion. It could also be useful in defining realistic boundary conditions for a more detailed cardiac model.

Acknowledgements

The authors acknowledge the *EUREKA-ADAPTER project* for funding this research work and also CIC-IT members and Sorin engineers for fruitful discussions.

References

[1] Leclerq C, Kass DA. Retiming the failing heart: principles and current clinical status of cardiac resynchronization. J. Am. Coll. Cardiol, 2002; vol. 39; 194-201.

[2] Whinnet ZI et al. Haemodynamic effects of changes in atrioventricular and interventricular delay in cardiacynchronization therapy show a consistent pattern:analysis of shape, magnitude and relative importance of atrioventricular and interventricular delay. Heart, Nov 2006; vol. 92; 1628-1634.

[3] Whinnet ZI et al. Determination of optimal atrioventricular delay for cardiac resynchronization therapy using acute non-invasive blood pressure. Europace, May 2006; vol. 6; 358-366.

[4] Hernandez AI et al. Overview of CARMEM: A new dynamic quantitative cardiac model for ecg monitoring and its adaptation to observed signals. Acta Biotheoretica, 2000; 48; 303-322.

[5] Smith BW et al. Minimal Haemodynamic system model including ventricular interaction and valve dynamics. Med Eng & Physics, 2004; 26; 131-139.

[6] Smith BW et al. Simulation of cardiovascular system diseases by including the autonomic nervous system into a minimal model. Computer methods and programs in biomedicine, 2007; 86; 153-160.

[7] Guarini M et al. Estimation of cardiac function from computer analysis of the arterial pressure waveform. IEEE transactions on biomed eng, Dec. 1998; **VOL. 45, NO. 12**, 1420.

[8] Santamore WP and Burkhoff D. Haemodynamic consequences of ventricular interaction as assessed by model analysis. Am J Physiol Heart Circ Physiol, Jan 1991; 260: H146 - H157.

[9] Jansen AH et al. Correlation of echo-Doppler optimzation of atrioventricular delay in cardiac resynchronization therapy with invasive hemodynamics in patients with heart failure secondary to ischemic or idiopathic dilated cardiomyopathy. Am J Cardiol, Feb 2006; 97; 552-557.

[10] Goldberg DE. Genetic Algorithms in search, optimization and machine learning. Boston, 1989.